http://journal.uir.ac.id/index.php/JGEET

E-ISSN: 2541-5794
P-ISSN : 2503-216X

Journal of Geoscience,
Engineering, Environment, and Technology
Vol 11 No 1 2026

RESEARCH ARTICLE

Correlation Between Land Cover Change and the Spatial Distribution of Land Surface Temperature in Tanjungpinang City, Indonesia

Arie Afriadi [1,*], Ghenady Septio[2], Aria Bagiasa Chidmahdjati[1] Dea Rizky Saputri[1]

[1] *Department of Urban and Regional Planning, Raja Ali Haji Maritime University, Indonesia*
[2] *Department of Geological Engineering, Gadjah Mada University, Indonesia*

* Corresponding Author: arieafriadi23@gmail.com
Received: Oct 1, 2016; Accepted: Mar 13, 2026.
DOI: 10.25299/jgeet.2026.11.1.22825

Abstract

Land cover change is a global environmental issue driving the Urban Heat Island (UHI) effect, in which artificial surfaces experience higher temperatures than vegetated areas. Tanjungpinang City, the capital of the Riau Islands Province, has experienced rapid development driven by population growth, leading in the conversion of green spaces into settlements and infrastructure and increasing urban heat island (UHI) risks. This study analyzes changes in land cover and land surface temperature (LST) from 2003 to 2023 and examines their Correlation. Using Google Earth Engine (GEE), we processed Landsat and MODIS imagery and used correlation analysis to assess the relationship between land cover changes and land surface temperature (LST) dynamics. The results of the study indicate that during the 2003–2023 period, Built-up Land experienced a significant increase of 27.15 km^2, which inversely correlated with a reduction in Vegetation area by 14.02 km^2. This transformation triggered an expansion of areas categorized under high and very high land surface temperatures in Tanjungpinang City. Correlation and regression analyses confirm a strong negative relationship between Vegetation and LST, underscoring vegetation's crucial role in reducing heat through shading and evapotranspiration. Conversely, Built-up Land shows a strong positive correlation with LST, highlighting its contribution as a primary driver of surface heat. Meanwhile, Water Bodies and Bare Land exhibit more varied influences with relatively minor impacts on overall urban temperature fluctuations. In general, this research concludes that the conversion of vegetated land to Built-up Land is the main factor driving increases in surface temperatures in Tanjungpinang City. These findings are expected to serve as a strategic foundation for the local government in evaluating spatial planning policies and prioritizing the integration of Green Open Spaces to achieve sustainable urban planning that is adaptive to climate change.

Keywords*:* Correlation, Land Cover (LC), Land Surface Temperature (LTS), Urban Heat Island (UHI)

1. Introduction

The dynamics of land cover change have become a critical issue in global environmental studies due to their significant role in degrading urban environmental quality (Ahmad et al., 2023). The conversion of natural land into built-up areas has been proven to directly contribute to increases in Land Surface Temperature (LST) (Rangel-Peraza et al., 2024). LST is a crucial physical environmental parameter, as it represents the energy exchange between the Earth's surface and the atmosphere through heat storage and release mechanisms (Zhu et al., 2023). In the context of global climate change, LST monitoring is widely used as a primary indicator to understand surface responses to environmental changes at the local scale. Widespread and uncontrolled increases in LST may trigger the Urban Heat Island (UHI) effect, in which urban areas experience significantly higher temperatures than surrounding regions with natural or rural land cover (Kafy et al., 2021).

Technically, the relationship between land cover change and LST is influenced by differences in physical properties and heat absorption capacities among land cover types (Vujovic et al., 2021). Natural surfaces, such as vegetation and water bodies, have high evapotranspiration capacity, which contributes to natural cooling despite their relatively low solar reflectance (Irawandani et al., 2018). In contrast, urbanization replaces vegetation with impervious surfaces such as concrete and asphalt, which have high heat-storage capacity and slowly release heat (Chatterjee & Majumdar, 2022). These materials absorb solar energy during the day and gradually release it at night, allowing high temperatures to persist for more extended periods (S. W. Wang et al., 2021). This condition is further exacerbated by urban form and building density, which hinder air circulation and promote heat accumulation in highly developed areas (Voogt & Oke, 2003).

Numerous studies have shown that landscape patterns and spatial structure strongly influence the spatial distribution of LST. Vegetation generally exhibits a strong inverse relationship with surface temperature, where higher vegetation density corresponds to lower surface temperatures (Guha & Govil, 2020). However, in tropical regions, surface heat levels are not solely influenced by vegetation but are also affected by air humidity and building density (Adeyeri et al., 2024). Such thermal imbalances result in decreased environmental comfort, increased energy consumption for cooling, and heightened risks of health-related issues (J. Wang et al., 2023; Ouria et al., 2025)

Tanjungpinang City, as the capital of the Riau Islands Province, represents a relevant study area due to its coastal characteristics influenced by land–sea interactions. Land

and sea breeze mechanisms play a vital role in regulating temperature dynamics, making even minor land cover changes capable of significantly affecting land surface temperature fluctuations (Cheval et al., 2024). These conditions render Tanjungpinang City vulnerable to terrestrial heat accumulation that is not fully offset by natural cooling from sea breezes, thereby potentially intensifying the Urban Heat Island phenomenon. Furthermore, as a center of government and economic activity, Tanjungpinang City has experienced rapid changes in land use over the past two decades (Sudjana et al., 2024). This development has driven significant alterations in land cover, particularly through the conversion of green spaces into residential and built-up areas. Such changes not only reduce the availability of green open spaces, which play a crucial role in maintaining ecosystem balance, but also contribute to increased surface temperatures and overall environmental degradation (Jannah & Bioresita, 2023). The rise in surface temperatures resulting from land cover change has become an increasingly critical issue, especially in coastal areas, where urbanization and settlement expansion have been shown to intensify urban heat island effects and reduce urban thermal comfort (Siregar et al., 2019). As a strategically important coastal city in the development of the Riau Islands Province, land cover change and rising surface temperatures in Tanjungpinang require serious attention, as these processes affect not only local environmental conditions but also regional climate dynamics (Zhu et al., 2023). Therefore, understanding how land cover change influences land surface temperature in Tanjungpinang City is essential.

This study aims to analyze land cover change and surface temperature distribution in Tanjungpinang City using remote sensing and Geographic Information Systems (GIS), supported by statistical analysis as a quantitative approach to data interpretation. This methodology has been widely applied in previous studies and has proven effective for monitoring environmental changes across large spatial scales (Wahyudi et al., 2018). The primary data sources used in this study consist of Landsat and MODIS satellite imagery, which are analyzed using land cover classification techniques and Land Surface Temperature (LST) analysis. Specifically, this study seeks to identify land cover change patterns over 20 years, with analysis points in 2003, 2013, and 2023. In addition, this research maps the distribution of surface temperatures by land cover type. It evaluates the relationship between land cover and surface temperature to understand the spatial Correlation between these two variables (Stamou et al., 2025).

This study is expected to provide insights into the impacts of land cover change on surface temperatures in Tanjungpinang City, serving as a foundation for improved regional planning and environmental management. Furthermore, the findings are expected to offer valuable recommendations for local governments and relevant stakeholders in formulating more sustainable urban spatial planning policies that are adaptive to climate change and support mitigation and adaptation efforts in response to rising temperatures driven by land cover change (Alisjahbana & Murniningtyas, 2018).

The study area is located in Tanjungpinang City, Riau Islands Province, along the coastline of Bintan Island (Figure 1). Geographically, it lies between 0°55′00″–1°10′00″ N and 104°23′00″–the Natuna Sea borders 104°35′00″ E. Tanjungpinang City to the north and south, and Bintan Regency to the east and west. Administratively, the city covers approximately 150 km^2 (BPS Tanjungpinang, 2023) and consists of four districts: Bukit Bestari, Tanjungpinang Barat, Tanjungpinang Kota, and Tanjungpinang Timur.(BPS Tanjungpinang, 2023).

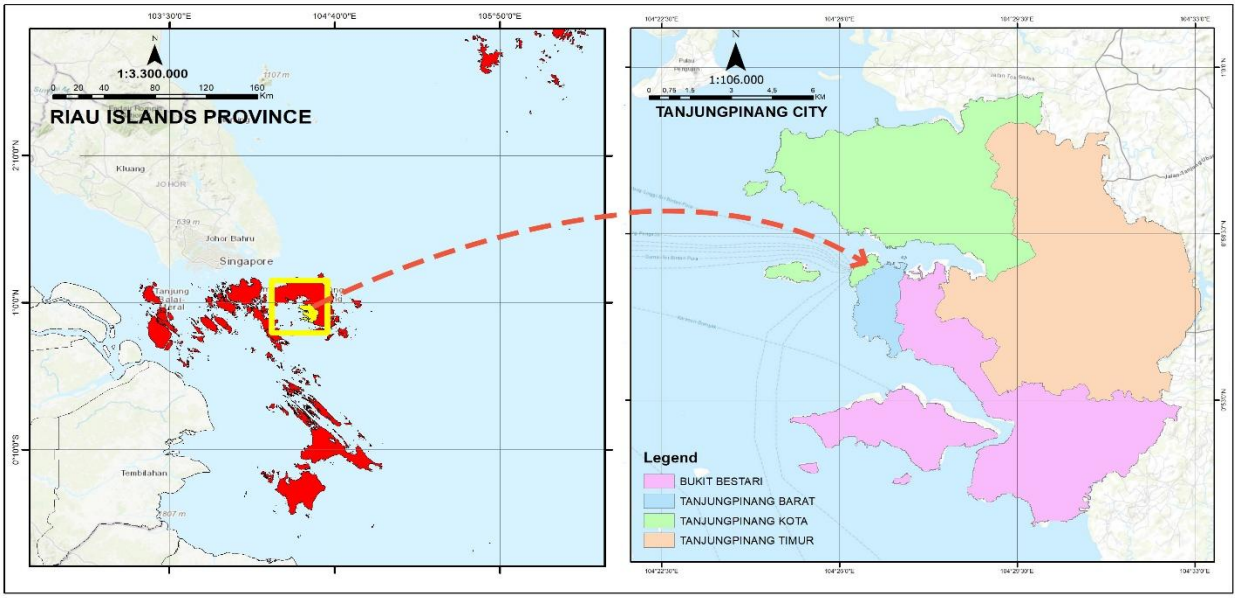

Fig 1. Research Area

2. Materials and Methods

This research employed a laptop equipped with ArcGIS 10.8 and QGIS 3.34 for spatial analysis, Microsoft Office 2019 for document processing, and Google Earth Engine (GEE) for cloud-based geospatial analysis and visualization. Access to GEE was obtained through its official web platform (https://earthengine.google.com/), which allows users to conduct advanced remote sensing and geospatial data processing directly in the cloud using its integrated JavaScript and Python APIs.

The datasets used in this study included Landsat 5 TM imagery (2003), Landsat 8 OLI imagery (2013 and 2023), MODIS imagery (2003, 2013, and 2023), the Tanjungpinang City Administrative Map, and the Indonesian Topographic Map (RBI). These datasets were selected for their relevance

to the analysis of land cover change using remote sensing and GIS techniques.

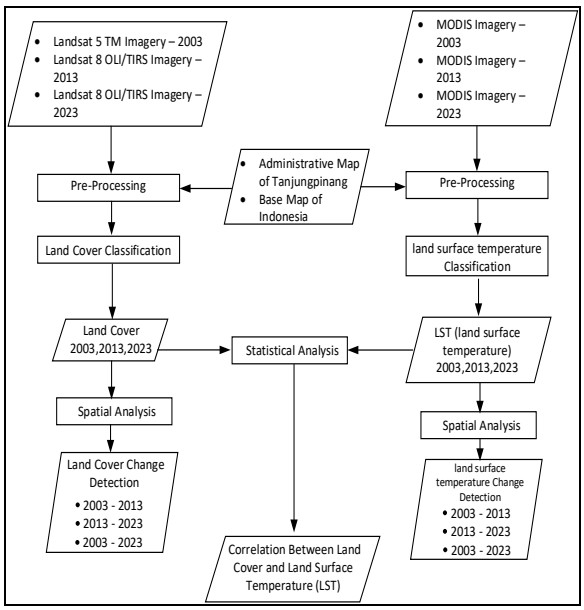

Fig 2. Framework diagram

2.1 Pre-Processing

The pre-processing stage constitutes the initial step in Landsat satellite image processing, preceding the primary analysis. This phase involves radiometric correction to enhance visual quality and spectral pixel accuracy (Handayani et al., 2017), followed by cropping Landsat and MODIS imagery to match the study area boundaries.

A. Radiometric Correction

Radiometric correction was performed using Google Earth Engine (GEE) for both Landsat 5 Thematic Mapper (TM) and Landsat 8 Operational Land Imager (OLI) datasets. The correction process advanced to the Top of Atmosphere (TOA) reflectance level, converting Digital Number (DN) values into reflectance values that represent surface energy reflection above the atmosphere (Wulder et al., 2022). This critical step improves spectral accuracy, reduces atmospheric interference, and ensures data consistency for subsequent analysis.

B. Band Compositing

Following TOA reflectance correction, multispectral band compositing integrates spectral channels into a single composite image, providing a comprehensive representation of surface features and facilitating more straightforward interpretation (Kalamkar & Geetha Mary, 2023). For Landsat 5-TM, bands 1 (blue), 2 (green), 3 (red), 4 (NIR), 5 (SWIR-1), and 7 (SWIR-2) were combined. Landsat 8-OLI utilized bands 1 (coastal), 2 (blue), 3 (green), 4 (red), 5 (NIR), 6 (SWIR-1), and 7 (SWIR-2).

C. Resampling

The difference in spatial resolution between land cover data derived from Landsat imagery, which has a spatial resolution of 30 meters (Alfiansyah et al., 2023), and Land Surface Temperature (LST) data from MODIS, with a spatial resolution of 1 kilometer (Yoo et al., 2020), requires a resolution harmonization step before further analysis. Therefore, a resampling process was applied during data pre-processing. The MODIS LST data, initially available at 1 kilometer, were resampled to 30 meters to match the Landsat imagery resolution. This resampling was conducted in ArcMap 10.8 using bilinear interpolation, which is appropriate for continuous data such as land surface temperature. Bilinear interpolation calculates new pixel values as a weighted average of surrounding pixels, resulting in a smoother, more representative temperature surface (Livada et al., 2023). This resampling step aligns the spatial units of analysis between the LST and land cover data, enabling subsequent analyses to be conducted consistently.

D. Image Cropping

The final pre-processing step involved cropping the composited Landsat 5-TM, Landsat 8-OLI, and MODIS images using ArcMap 10.8 to focus exclusively on Tanjungpinang City's administrative boundaries, optimizing data processing efficiency and analytical relevance.

2.2 Land Cover Classification and Land Surface Temperature Analysis

A. Land Cover Classification

Land cover classification was performed using a supervised classification approach. Supervised classification is a digital image processing method that identifies and categorizes pixels into specific classes based on their spectral characteristics (Egorov et al., 2015). A commonly employed technique is Maximum Likelihood Classification (MLC), which assumes that the spectral distribution of each class follows a distinct pattern. This method assigns pixel membership to a particular class based on the highest probability, using statistical estimates such as mean vectors and covariance matrices derived from training samples. The accuracy of classification heavily depends on the representativeness of the training data, as improper estimation can lead to less precise results (Lu et al., 2003).

Land cover classification was performed using a supervised classification method, with training areas manually identified from visual interpretation of composited Landsat imagery, taking topographic map information into account. The user selected representative areas for each land cover class, such as built-up areas, water bodies, vegetation, and bare land (Moraes et al., 2024). From these areas, several pixels were chosen as training samples based on similarity in tone, color, and texture (Seyam et al., 2023; Farnaz et al., 2025). These samples were then analyzed on the imagery to obtain the statistical information required for the classification process. To ensure consistent and accurate results, training areas were selected from regions with high homogeneity.

B. Land Surface Temperature (LST) classification

Land Surface Temperature (LST) classification groups surface temperature distributions into several classes based on specific value ranges. The primary purpose of this classification is to facilitate spatial analysis of heat distribution across a given area (Kurniantoro et al., 2023).

The classification process is carried out through reclassification steps based on pixel temperatures from MODIS satellite imagery for 2003, 2013, and 2023. These temperature values are then categorized into five classes.

Table 1. Classification & Value LST (Ally et al., 2024)

Classification	Value LST
Class 1	< 25^0 C
Class 2	25,1^0 C - 28^0 C
Class 3	28,1^0 C - 30^0 C
Class 4	30,1^0 C - 32^0 C
Class 5	> 32,1^0 C

2.3 Analysis of Land Cover Change and LST Change

Analysis of Land Cover Change and Land Surface Temperature (LST) Change Using the Overlay Technique. The overlay technique is a spatial analysis method that combines multiple spatial data layers with the same geographic reference to generate new information (Zhao et al., 2019). In the context of Geographic Information Systems (GIS), overlay techniques are used to systematically and structurally identify spatial changes that occur over time (Anasiru, 2016; Hermosilla et al., 2022).

In this study, the overlay technique was used to map land cover changes and Land Surface Temperature (LST) changes across two time periods: 2003-2013 and 2013-2023. The overlay process was conducted pairwise for each period to identify spatial changes in each land cover class. Through this process, information was obtained regarding land cover dynamics, revealing shifts in land use classes within specific areas over time (Rosandi et al., 2024).

The exact process was applied to LST data that had previously been classified. Subsequently, overlay analysis was performed for both periods. The results show the spatial distribution of areas experiencing either increases or decreases in surface temperature.

2.4 Analysis of the Influence of Land Cover Change on Land Surface Temperature

Analysis of the Influence of Land Cover Change on Land Surface Temperature Using Statistical Approaches. The study employs two main statistical approaches: correlation analysis and regression analysis, aimed at understanding the relationship between land cover variables and Land Surface Temperature (LST) (Noviani et al., 2024). The study was conducted separately for each observation year (2003, 2013, and 2023) to examine the dynamics and patterns of variable relationships across periods independently.

A. Correlation Analysis

Correlation analysis was used to assess the strength of association between land cover and LST for each year. This analysis does not infer causation but instead evaluates the direction and strength of the relationship between variables (Eboy & Kemarau, 2023).

$$(\boldsymbol{x}, \boldsymbol{y}) = \frac{\boldsymbol{n}\sum \boldsymbol{xy} - \sum \boldsymbol{x} \sum \boldsymbol{y}}{\sqrt{[\boldsymbol{n}\sum \boldsymbol{x^2} - (\sum \boldsymbol{x})^2][\boldsymbol{n}\sum \boldsymbol{y^2} - (\sum \boldsymbol{y})^2]}} \quad (1)$$

r = Correlation Coefficient
x = Independent Variable
y = Dependent Variabel
n = Banyaknya Pengamatan

The value of r indicates a positive relationship if an increase in one variable is followed by a rise in the other, a negative relationship if an increase in one variable is followed by a decrease in the other, and a value close to zero if no linear relationship exists between the variables. In short, the correlation coefficient helps determine both the direction and strength of the relationship between two variables (Alexander, 2020). Additionally, the magnitude of r reflects the strength of this relationship: values between 0.00 and 0.199 are considered very weak, 0.20 and 0.39 as weak, 0.40 and 0.59 as moderate, 0.60 and 0.79 as strong, and 0.80 and 1.00 as very strong (Table 2).

Table 2. Correlation Coefficient Criteria (Siregar et al., 2019)

Correlation coefficient	Classification
0,00 – 0,199	Very Weak
0,20 – 0,399	Weak
0,40 – 0,599	Moderate
0,60 – 0,799	Stong
0,80 – 1,000	Very Strong

B. Regression Analysis

Regression analysis was used to statistically model the influence of land cover changes on Land Surface Temperature (LST) for each observed year (Nurwanda & Honjo, 2020). This model not only examines the relationships between variables but also quantifies the contribution of each land cover class, such as built-up areas, vegetation, water bodies, and bare land, to local surface temperature (LST) values. Through this analysis, we can identify which land cover class has the most significant impact on annual changes in surface temperature.

The regression results reveal the extent to which each land cover class contributes to variations in surface temperature, providing a clearer understanding of the relationship between land cover changes and surface temperature patterns in Tanjungpinang City.

$$Y = a + bX \quad (2)$$

Y = Dependent Variable

X = Independent Variable

a = Constant (intercept)

b = Regression Coefficient (Slope)

3. Results & Discussion

3.1 Pre-Processing

Pre-processing of Landsat and MODIS imagery was performed using the Google Earth Engine (GEE) platform (https://earthengine.google.com/). Landsat data processing included defining the Region of Interest (ROI), selecting imagery based on temporal criteria, converting data to Top of Atmosphere (TOA) reflectance, generating band composites, and exporting the processed images. This workflow was consistently applied for the observation years 2003, 2013, and 2023. For MODIS imagery, pre-processing involved defining the ROI, determining the observation period, and calculating annual mean Land Surface Temperature (LST) values. Figure 3 presents a representative GEE script illustrating the processing workflow. The complete set of Google Earth Engine scripts used in this study is available at https://bit.ly/4bqR4it.

```
// Mendefinisikan ROI (Polygon) yang digunakan
var ROI = ee.Geometry.Polygon([
  [
    [104.36079374934832, 0.8242373465108328],
    [104.56404081966082, 0.8242373465108328],
    [104.56404081966082, 0.9986231718896573],
    [104.36079374934832, 0.9986231718896573],
    [104.36079374934832, 0.8242373465108328]
  ]
]);

// Mendapatkan citra Landsat 8 (OLI/TIRS) untuk tahun 2022-2023
var dataset = ee.ImageCollection('LANDSAT/LC08/C02/T1')
  .filterBounds(ROI) // Filter berdasarkan ROI
  .filterDate('2022-01-01', '2023-12-31'); // Rentang waktu

print(dataset, 'Dataset');

// Mengambil citra spesifik berdasarkan ID
var single = ee.Image('LANDSAT/LC08/C02/T1/LC08_125059_20230725');
print(single, 'Selected Image');

var potong = single.clip(ROI); // Memotong citra dengan ROI

// Menghitung TOA (Top of Atmosphere) untuk citra
var TOA = ee.Algorithms.Landsat.TOA(potong); // Koreksi TOA
var trueColor = TOA.select(['B4', 'B3', 'B2']); // Komposit True Color: Red (B4), Green (B3), Blue (B2)
Map.addLayer(trueColor, {min: 0, max: 0.3}, 'True Color (Landsat 8)');

// Menambahkan ekspor citra ke Google Drive
Export.image.toDrive({
  image: trueColor, // Komposit True Color
  description: 'TrueColor_Export', // Nama file ekspor
  scale: 30, // Resolusi (30m untuk Landsat)
  region: ROI, // Area yang akan diekspor
  fileFormat: 'GeoTIFF', // Format output
  maxPixels: 1e8 // Batas jumlah piksel
});
```

Fig 3. Script Pre-Processing

The results of the pre-processing stage are shown in Figure 4, which displays the image output after radiometric correction, band compositing, and clip/cropping. This pre-

processing provides an overview of the data condition, which is now ready for further analysis of both Landsat and MODIS imagery.

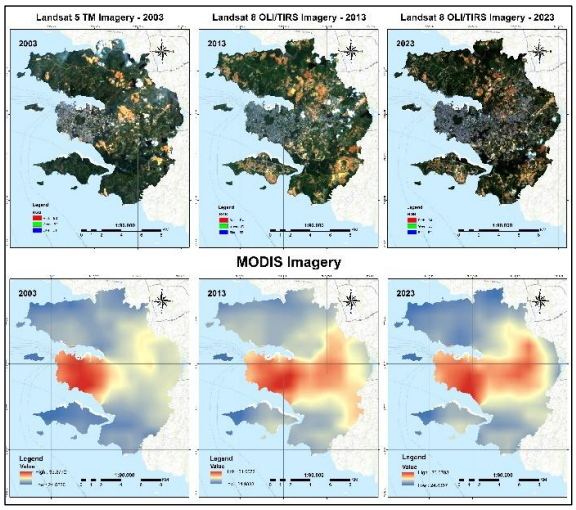

Fig 4. Landsat and MODIS Imagery Map

3.2 Land Cover Classification and LST Classification

A. Land Cover Classification

The land cover classification process was carried out by defining training sample areas. The greater the number of samples used, the higher the classification accuracy (Kausarian et al., 2023). Sample selection was based on land cover categories, including Water Bodies, Built-Up Areas, Bare Land, and Vegetation. Class grouping was performed through Landsat image interpretation using band combinations, taking into account visual characteristics such as texture, color, and pattern (Farnaz et al., 2025).

Table 3. Land cover training sample Area

Land Cover	Training Sampel Area	Band Combination L 5 TM	Band Combination L 8 OLI	Description
Water Bodies		4,3,2	5,4,3	The water body is a combination of waters in the form of rivers, lakes and reservoirs, based on a combination of 543, which is pitch black in color with a smooth texture.
Bare Land		7,4,2	7,5,3	Bare land is dry land that does not contain elements of vegetation development and growth, based on a combination of 753 colors it is light brown.
Built-up Land	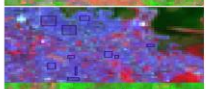	2,4,5	5,3,6	Built-up land is a combination of residential areas, buildings and roads, based on the combination of 536 in blue.
Vegetation		7,4,2	7,5,3	Vegetation is green land covered with forests, bushes, or gardens. In the combination of band 753, the vegetation area appears bright green.

The subsequent process involved conducting Maximum Likelihood Classification (MLC) analysis based on land cover training sample categories for Landsat imagery from 2003, 2013, and 2023. A classification smoothing process was then applied to minimize pixel-level errors in the analysis. The final classification results for all three years (2003, 2013, and 2023) are presented in Figure 5.

Based on land cover classifications conducted in 2003, 2013, and 2023, the results show that in 2003, the area of water bodies was 4.54 km^2, accounting for approximately 3.02% of the total area. This area increased in 2013 to 4.88 km^2 (3.24%) but decreased again in 2023 to 4.15 km^2 (2.76%). Built-up land exhibited a significant increasing trend, from 11.34 km^2 (7.54%) in 2003 to 25.34 km^2 (16.85%) in 2013, and continued to rise to 38.49 km^2 (25.59%) in 2023. Meanwhile, bare land increased slightly from 23.75 km^2 (15.79%) in 2003 to 25.21 km^2 (16.76%) in 2013, but then declined sharply to 11.02 km^2 (7.33%) in 2023. Vegetation cover, which represented the largest land cover category, decreased from 110.75 km^2 (73.64%) in 2003 to 94.96 km^2 (63.14%) in 2013. Although the vegetation area increased slightly to 96.73 km^2 (64.32%) in 2023, the overall trend still indicates a decline compared to the initial year of observation.

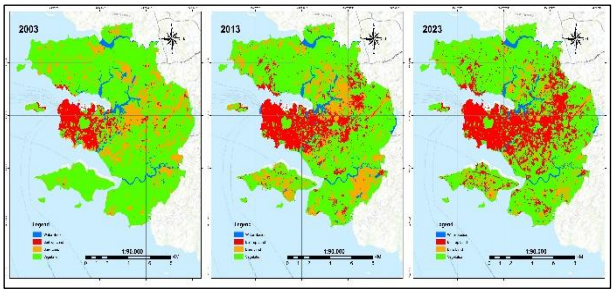

Fig 5. Classification results of Landsat imagery for 2003, 2013 and 2023

Table 4. Land Cover Change in 2003, 2013, and 2023

Year	Land Cover	Area (Km^2)	Percentage (%)
2003	Water Bodies	4.54	3.02
	Built-up Land	11.34	7.54
	Bare Land	23.75	15.79
	Vegetation	110.75	73.64
	Total	150.38	100.00
2013	Water Bodies	4.88	3.24
	Built-up Land	25.34	16.85
	Bare Land	25.21	16.76
	Vegetation	94.96	63.14
	Total	150.38	100.00
2023	Water Bodies	4.15	2.76
	Built-up Land	38.49	25.59
	Bare Land	11.02	7.33
	Vegetation	96.73	64.32
	Total	150.38	100.00

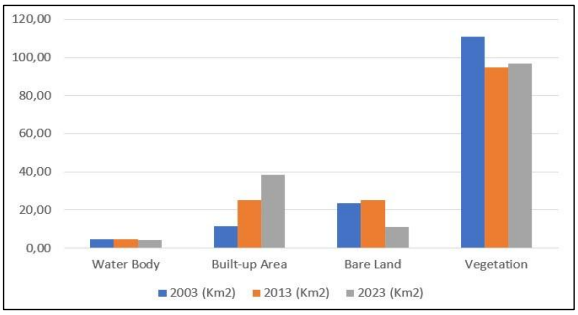

Fig 6. Land Cover Change Graph for 2003, 2013, and 2023

B. Land Surface Temperature (LST) classification

The Land Surface Temperature (LST) classification was performed by reclassifying MODIS image pixel values into five temperature categories (Zhang et al., 2022). The first class, designated as very low temperature, comprises values below 25°C. The second class (low temperature) ranges from 25.1°C to 28°C. The third category, classified as moderate temperature, encompasses values between 28.1°C and 30°C. Subsequently, the high temperature class covers the range from 30.1°C to 32°C. Finally, the exceptionally high temperature category includes all values exceeding 32°C.

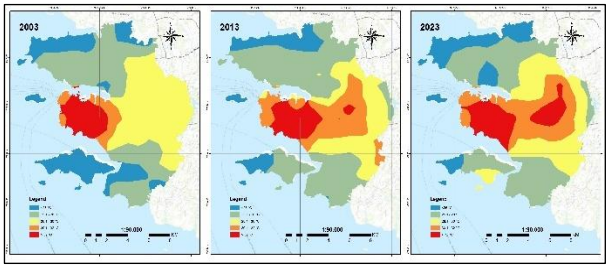

Fig 7. Classification results of the Land Surface Temperature (LST) for 2003, 2013, and 2023

Based on the classification results of Land Surface Temperature (LST) in 2003, 2013, and 2023, there has been a significant dynamic change in surface temperature over the past two decades. In 2003, the very low temperature class (<25 °C) covered 31.55 km^2, but declined to 15.58 km^2 in 2013, before increasing again to 20.66 km^2 in 2023. The low temperature class (25.1–28 °C) showed an increase from 50.31 km^2 in 2003 to 66.25 km^2 in 2013, but then decreased to 50.98 km^2 in 2023. Meanwhile, the moderate temperature class (28.1–30 °C) experienced a sharp decline from 49.57 km^2 in 2003 to 30.07 km^2 in 2013, with a slight increase to 34.60 km^2 in 2023. The high-temperature class (30.1–32 °C) exhibited a significant upward trend, increasing from 7.22 km^2 in 2003 to 25.92 km^2 in 2013, and remained relatively stable in 2023 at 25.95 km^2. The very high temperature class (>32°C) also showed a gradual increase, from 11.73 km^2 in 2003 to 12.55 km^2 in 2013, and further to 18.19 km^2 in 2023. Overall, these results suggest a consistent trend of increasing land surface temperatures.

Table 5. Temperature Changes in 2003, 2013, and 2023

Year	LST (°C)	Description	Area (Km^2)	Percentage (%)
2003	<25 °C	Very Low	31.55	20.98
	25.1 - 28 °C	Low	50.31	33.46
	28.1 - 30 °C	Moderate	49.57	32.96
	30.1 - 32 °C	High	7.22	4.80
	> 32 °C	Very High	11.73	7.80
	Total		150.38	100.00
2013	< 25 °C	Very Low	15.58	10.36
	25.1 - 28 °C	Low	66.25	44.06
	28.1 - 30 °C	Moderate	30.07	20.00
	30.1 - 32 °C	High	25.92	17.24
	> 32 °C	Very High	12.55	8.35
	Total		150.38	100.00
2023	< 25 °C	Very Low	20.66	13.74
	25.1 - 28 °C	Low	50.98	33.90
	28.1 - 30 °C	Moderate	34.60	23.01
	30.1 - 32 °C	High	25.95	17.25
	> 32 °C	Very High	18.19	12.10
	Total		150.38	100.00

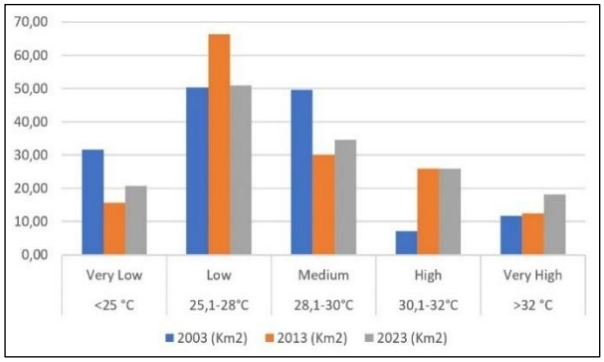

Fig 8. Temperature Change Graph for 2003, 2013, and 2023

3.3 Changes in Land Cover and Land Surface Temperature (LST)

A. Land Cover Change

Land cover changes observed during the periods 2003–2013, 2013–2023, and the entire span from 2003 to 2023 reflect dynamic patterns of spatial utilization and significant transformations in the physical landscape of the study area. The most notable change occurred in built-up land, which increased by 14.01 km^2 between 2003 and 2013 and by 13.14 km^2 from 2013 to 2023. This growth amounts to a total increase of 27.15 km^2 over the last two decades, indicating rapid urbanization and development, likely driven by population growth, infrastructure expansion, and socio-economic development. In contrast, vegetation cover declined sharply by 15.79 km^2 during the first decade, followed by a modest recovery of 1.77 km^2 between 2013 and 2023. Despite this slight regrowth, the overall reduction in vegetation cover reached 14.02 km^2, highlighting ongoing ecological pressure from land conversion and reduced green space.

Bare land exhibited a different trend. It initially increased by 1.45 km^2 from 2003 to 2013, likely due to deforestation or land clearing activities. However, over the following decade, bare land decreased by 14.19 km^2, resulting in a net reduction of 12.74 km^2. This pattern suggests that areas once left exposed were subsequently developed into built-up zones. Meanwhile, water bodies experienced only minor fluctuations, increasing slightly by 0.33 km^2 in the first decade and decreasing by 0.72 km^2 in the second. Overall, water bodies declined by 0.39 km^2, a relatively small but notable change, indicating alterations in aquatic systems potentially due to land reclamation, sedimentation, or climate-related factors. Together, these trends illustrate the spatial and ecological transformation of the landscape, shaped by both anthropogenic pressures and natural processes (Bogaert et al., 2014).

Table 6. Land Cover Area Difference

Land Cover	Year	Year	Year	difference	difference	difference
	2003	2013	2023	2003 & 2013	2013 & 2023	200 & 2023
Water Bodies	4.54	4.88	4.15	0.33	-0.72	-0.39
Built-up Land	11.34	25.34	38.49	14.01	13.14	27.15
Bare Land	23.75	25.21	11.02	1.45	-14.19	-12.74
Vegetation	110.75	94.96	96.73	-15.79	1.77	-14.02

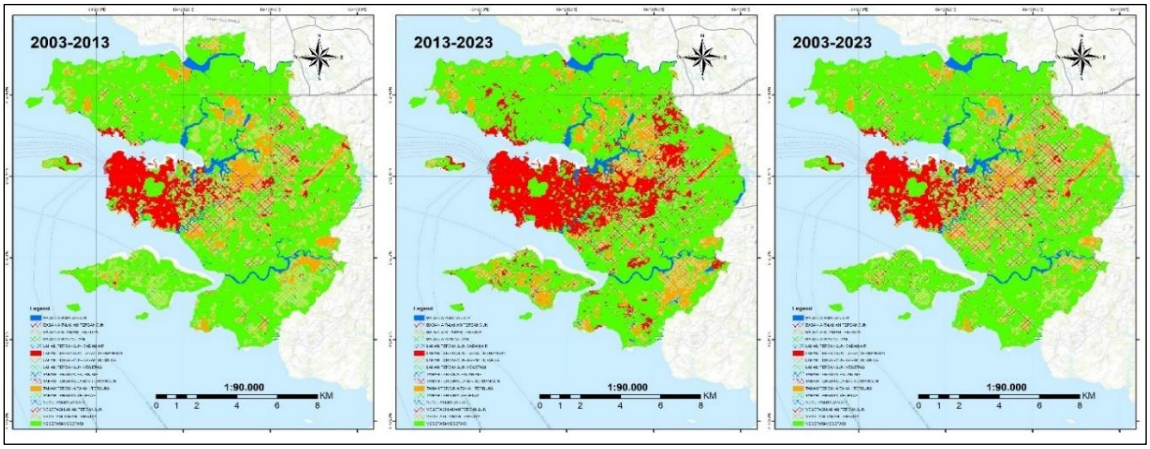

Fig 9. Land Cover Change Map 2003, 2013, & 2023

A more detailed examination at the district scale indicates that land cover changes exhibit diverse spatial patterns, reflecting differences in regional functions and development intensity among districts. Bukit Bestari District experienced a consistent increase in built-up land, from 3.93 km^2 (9%) in 2003 to 7.23 km^2 (16%) in 2013, and further expanding to 10.11 km^2 (22%) in 2023. This growth was accompanied by a substantial decline in vegetation cover during the initial period, decreasing from 36.13 km^2 (80%) to 26.60 km^2 (59%). Although vegetation cover partially recovered in 2023 to 29.54 km^2 (66%), Bukit Bestari remains an area under considerable urbanization pressure, while still retaining relatively better green space potential compared to districts with higher levels of built-up development.

In contrast, Tanjungpinang Barat District has been dominated by built-up land since the early period of observation. In 2003, built-up areas accounted for 77% of the district, rising to 90% in 2013 and 91% in 2023. Vegetation cover in this district is minimal and relatively stagnant, remaining at approximately 9–14% over the two-decade period. The very high dominance of built-up land characterizes this district as the urban core, with a mature level of urbanization and a limited capacity to mitigate environmental impacts associated with intensified urban activities.

Meanwhile, Tanjungpinang Kota District exhibits more moderate land cover changes. Built-up land increased gradually from 1.29 km^2 (3%) in 2003 to 3.70 km^2 (9%) in 2023. Vegetation remained the dominant land cover type, accounting for more than 75% of the area throughout the study period, despite minor fluctuations. This condition suggests that Tanjungpinang Kota District has maintained a balance between urban development and vegetation cover, potentially contributing to greater stability in surface environmental conditions.

The most dynamic changes occurred in Tanjungpinang Timur District, where built-up land expanded sharply from 2.62 km^2 (4%) in 2003 to 11.49 km^2 (19%) in 2013, and increased further to 20.56 km^2 (33%) in 2023. This expansion coincided with a decline in vegetation cover from 41.65 km^2 (68%) to 35.17 km^2 (57%). These patterns indicate that Tanjungpinang Timur has emerged as a new urban expansion zone, characterized by intensive land conversion from vegetated and open areas into built-up land (Saputri et al., 2025). Overall, the inter-district variation in land cover change confirms that urbanization processes within the study area are spatially uneven, and differences in land cover structure play a critical role in explaining spatial variations in land surface temperature (Mohamed et al., 2025). A summary of land cover distribution and dynamics across districts is presented in Table 7, while the spatial patterns of land cover change are illustrated in Figure 10.

Table 7. Land Cover Change by District

Year	Land Cover	Bukit Bestari District		Tanjungpinang Barat District		Tanjungpinang Kota District		Tanjungpinang Timur District	
		Area (Km^2)	Percentage (%)	Area (Km^2)	Percentage (%)	Area (Km^2)	Percentage (%)	Area (Km^2)	Percentage (%)
2003	Water Bodies	1,07	2%	0,03	1%	1,55	4%	1,90	3%
	Built-up Land	3,93	9%	3,50	77%	1,29	3%	2,62	4%
	Bare Land	3,81	8%	0,36	8%	4,34	11%	15,25	25%
	Vegetation	36,13	80%	0,65	14%	32,31	82%	41,65	68%
	Total	44,94	100%	4,53	100%	39,49	100%	61,42	100%
2013	Water Bodies	1,31	3%	0,01	0%	1,65	4%	1,91	3%
	Built-up Land	7,23	16%	4,09	90%	2,53	6%	11,49	19%
	Bare Land	9,80	22%	0,03	1%	5,35	14%	10,02	16%
	Vegetation	26,60	59%	0,41	9%	29,95	76%	38,00	62%
	Total	44,94	100%	4,53	100%	39,49	100%	61,42	100%
2023	Water Bodies	1,02	2%	0,00	0%	1,48	4%	1,65	3%
	Built-up Land	10,11	22%	4,12	91%	3,70	9%	20,56	33%
	Bare Land	4,28	10%	0,00	0%	2,69	7%	4,04	7%
	Vegetation	29,54	66%	0,41	9%	31,62	80%	35,17	57%
	Total	44,94	100%	4,53	100%	39,49	100%	61,42	100%

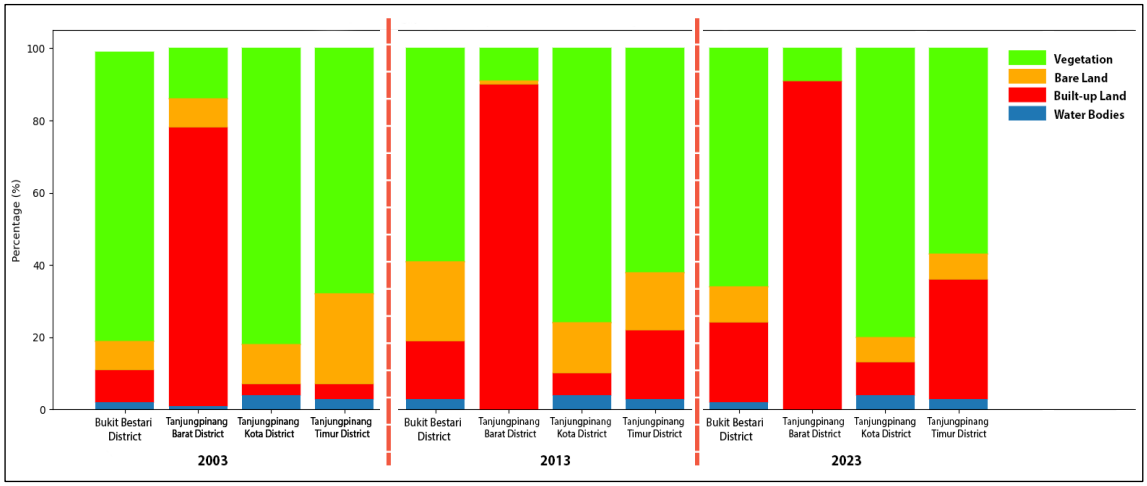

Fig 10. Land Cover Change by District

B. Land Surface Temperature Change

The analysis of Land Surface Temperature (LST) changes from 2003 to 2013, 2013 to 2023, and overall from 2003 to 2023 reveals thermal dynamics that reflect changes in land cover and anthropogenic activities. The Very Low temperature category (<25°C) experienced a significant decrease of 15.97 km^2 from 2003 to 2013, followed by an increase of 5.08 km^2 in the subsequent decade; however, it still showed an overall decline of 10.89 km^2. Meanwhile, the Low category (25.1–28°C) increased by 15.94 km^2 in the first decade but then sharply declined by 15.27 km^2 in the following decade, resulting in a relatively minor net change of +0.67 km^2. The Moderate category (28.1–30°C) experienced a substantial reduction of 19.50 km^2 from 2003 to 2013, followed by a modest increase of 4.53 km^2, resulting in a total decrease of 14.97 km^2. The high-temperature category (30.1–32°C) expanded by 18.71 km^2 between 2003 and 2013, remaining relatively stable thereafter, resulting in a cumulative increase of 18.73 km^2, indicating the spread of high-temperature areas. The Very High category (>32°C) exhibited a gradual rise, with an increase of 0.82 km^2 in the first decade and 5.64 km^2 in the second, resulting in a total addition of 6.46 km^2. This trend may reflect heat concentration in certain zones due to a reduction in green open spaces or the intensification of human activities.

Table 8. Land Surface Temperature Difference

LTS	Year	Year	Year	difference	difference	difference
	2003	2013	2023	2003 & 2013	2013 & 2023	2003 & 2023
<25 °C	31.55	15.58	20.66	-15.97	5.08	-10.89
25,1-28°C	50.31	66.25	50.98	15.94	-15.27	0.67
28,1-30°C	49.57	30.07	34.60	-19.50	4.53	-14.97
30,1-32°C	7.22	25.92	25.95	18.71	0.02	18.73
>32 °C	11.73	12.55	18.19	0.82	5.64	6.46

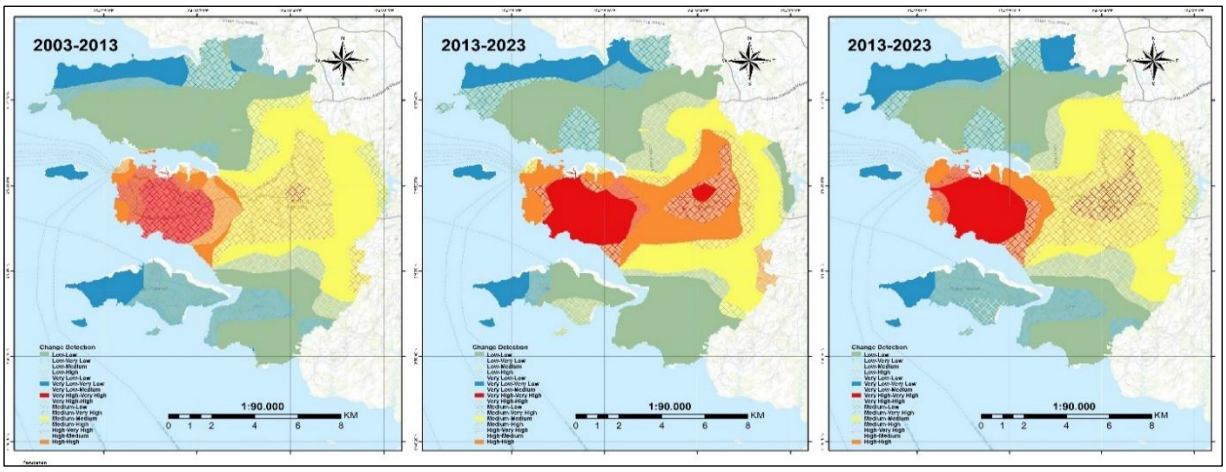

Fig 11. Land Surface Temperature Change Map 2003, 2013, and 2023

A further examination at the district scale indicates that the distribution and dynamics of Land Surface Temperature (LST) exhibit pronounced spatial contrasts, corresponding to differences in land cover composition and development intensity across districts. In 2003, Bukit Bestari District was predominantly characterized by low to moderate temperature classes, with the <25 °C and 25.1–28 °C categories accounting for more than 70% of the area. However, by 2013 and 2023, a clear shift toward higher temperature classes was observed, marked by an increase in the proportion of regions exceeding 32 °C from 15% in 2003 to 18% in 2023. This shift reflects intensified urban activity and a reduced capacity of the environment to

dissipate heat, although portions of the district still exhibited relatively low temperatures in vegetated areas.

Tanjungpinang Barat District displays the most extreme thermal characteristics among all districts. Since 2003, this district has been dominated by high- to very-high-temperature classes, with areas exceeding 32 °C accounting for 80% of the total area. Although this proportion declined in 2013 and 2023, the dominance of the 30.1–32 °C and >32 °C classes remained pronounced. These conditions indicate high development intensity, dense built-up structures, and limited green open spaces, which collectively contribute to persistent surface heat accumulation.

Tanjungpinang Kota District exhibits relatively more stable thermal conditions. In both 2003 and 2013, the district was dominated by low-to-moderate temperature classes, particularly within the 25.1–28 °C range. By 2023, the area with temperatures below 25 °C increased to 43%, highlighting the role of vegetation and water bodies in maintaining thermal balance. The absence of temperature classes exceeding 32 °C throughout the observation period further suggests that thermal pressure resulting from urban development in this district remains relatively controlled.

The most dynamic thermal changes occurred in Tanjungpinang Timur District. In 2003, this district was characterized by moderate temperatures (28.1–30 °C), which covered approximately 75% of the area. However, by 2013 and 2023, a significant shift toward high- and very-high-temperature classes was evident. In 2023, the combined extent of the 30.1–32 °C and >32 °C classes accounted for nearly half of the district area. This increase corresponds with the rapid expansion of built-up land, reinforcing indications of emerging urban heat zones within newly developed areas. Overall, inter-district differences in LST patterns confirm that areas dominated by built-up land and limited vegetation tend to experience higher and more persistent increases in surface temperature (Fathoni, 2025). Conversely, districts that retain relatively extensive vegetation cover exhibit more stable thermal conditions (Gomaa et al., 2025). The distribution of land surface temperature classes across districts is presented in Table 9, while the spatial patterns of LST change are illustrated in Figure 12.

Table 9. Land Surface Temperature Change by District

Year	LST (°C)	Bukit Bestari District		Tanjungpinang Barat District		Tanjungpinang Kota District		Tanjungpinang Timur District	
		Area (Km^2)	Percentage (%)	Area (Km^2)	Percentage (%)	Area (Km^2)	Percentage (%)	Area (Km^2)	Percentage (%)
2003	<25 °C	17,21	38%	0,00	0%	12,62	32%	1,72	3%
	25,1-28°C	15,98	36%	0,00	0%	25,65	65%	8,68	14%
	28,1-30°C	3,13	7%	0,00	0%	0,40	1%	46,05	75%
	30,1-32°C	2,10	5%	0,88	20%	0,77	2%	3,46	6%
	>32 °C	6,52	15%	3,65	80%	0,06	0%	1,50	2%
	Total	44,94	100%	4,53	100%	39,49	100%	61,42	100%
2013	<25 °C	4,06	9%	0,00	0%	10,49	27%	1,04	2%
	25,1-28°C	25,55	57%	0,00	0%	27,89	71%	12,82	21%
	28,1-30°C	5,83	13%	0,00	0%	0,62	2%	23,61	38%
	30,1-32°C	2,31	5%	3,29	72%	0,49	1%	19,83	32%
	>32 °C	7,19	16%	1,25	28%	0,00	0%	4,11	7%
	Total	44,94	100%	4,53	100%	39,49	100%	61,42	100%
2023	<25 °C	2,46	5%	0,00	0%	17,10	43%	1,10	2%
	25,1-28°C	23,70	53%	0,00	0%	19,23	49%	8,05	13%
	28,1-30°C	9,85	22%	0,00	0%	2,25	6%	22,50	37%
	30,1-32°C	0,89	2%	2,49	55%	0,90	2%	21,66	35%
	>32 °C	8,03	18%	2,04	45%	0,00	0%	8,12	13%
	Total	44,94	100%	4,53	100%	39,49	100%	61,42	100%

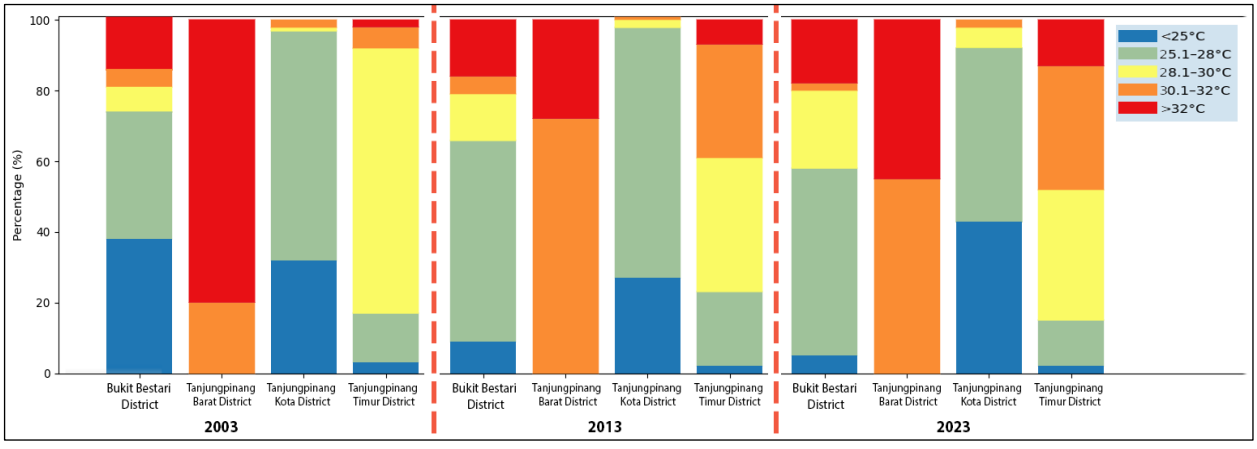

Fig 12. Land Surface Temperature Change by District

C. Correlation Between Land Cover and Land Surface Temperature (LST)

The correlation analysis between land cover and Land Surface Temperature (LST) in 2003 shows a strong relationship between land cover types and surface temperature variations, as demonstrated in both tabular data and regression graphs. Vegetation cover dominated the low-temperature categories, namely <25 °C and 25.1–28 °C, with respective areas of 28.98 km^2 and 42.50 km^2, and exhibited a strong negative correlation with LST (r = -0.80). This is also reflected in the LST-vegetation regression graph, where a negative regression coefficient (y = -2.2078x + 28.773) and a high R^2 value (0.6404) indicate a clear downward trend in LST with increasing vegetation cover.

This pattern aligns with vegetation's ability to reduce heat through solar radiation absorption and evapotranspiration. In contrast, built-up land showed a robust positive correlation with LST (r = 0.87), clearly illustrated in the regression graph (y = 1.5851x - 2.4874, R^2 = 0.7647), which displays a consistent upward temperature trend in line with the expansion of built-up areas, particularly in the high-temperature category (>32 °C), which reached an area of 7.16 km^2. Water bodies exhibited a moderate negative correlation (r = -0.51) and demonstrated a cooling trend as the area increased. The LST–water regression graph showed a negative slope (y = -0.2452x + 1.6441; R^2 = 0.2604), indicating that water tends to increase thermal stability in the region. Meanwhile, bare land showed a very weak relationship with LST (r = -0.14), and the regression line (y = -0.4916x + 6.2253, R^2 = 0.0200) showed an almost flat trend, suggesting an insignificant contribution to surface thermal dynamics, possibly due to heterogeneous characteristics and varying moisture conditions.

Overall, these regression patterns reinforce the finding that the conversion of vegetated areas into built-up land was the main driver of surface temperature increase in Tanjungpinang City in 2003 (Table 10 and Fig. 13).

Table 10. Correlation of Land Cover to Land Surface Temperature (LST) in 2003

	TAHUN 2003				
	LST (°C)	Water Bodies	Built-up Land	Bare Land	Vegetation
		KM²			
1	<25 °C	0.60	0.23	1.75	28.98
2	25,1-28°C	2.10	0.44	5.27	42.50
3	28,1-30°C	1.18	1.08	14.11	33.20
4	30,1-32°C	0.47	2.43	1.40	2.92
5	>32 °C	0.19	7.16	1.23	3.16
	correlation (r)	**-0.51**	**0.87**	**-0.14**	**-0.80**

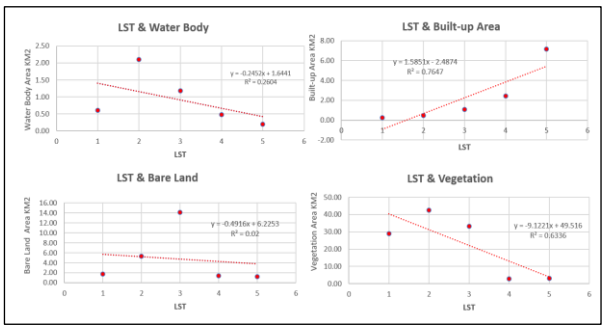

Fig 13. Graph of the Influence of Land Cover on Land Surface Temperature (LST) 2003

An analysis of the relationship between land cover and Land Surface Temperature (LST) in the year 2013 reveals a statistically significant association between land cover types and surface temperature variations. This relationship is illustrated through the spatial distribution table and the linear regression graph. Vegetation cover predominantly occurs in the lower-temperature categories, specifically within the <25 °C and 25.1–28 °C ranges, with respective areas of 11.44 km^2 and 49.56 km^2. Vegetation exhibits a negative correlation with LST (r = -0.48), modeled by the linear regression equation y = -5.5361x + 35.6, and a coefficient of determination R^2 = 0.2339. Although the R^2 value indicates moderate explanatory power, the inverse relationship between vegetation extent and surface temperature remains evident, highlighting the cooling influence of vegetated areas. In contrast, built-up land exhibits a strong positive correlation with LST (r = 0.88), as indicated by the regression equation y = 2.4859x - 2.3887 and an R^2 value of 0.7696. This strong Correlation underscores the significant impact of urban expansion on surface temperature dynamics. In the higher temperature categories (30.1–32 °C and >32 °C), the extent of built-up land reached 10.61 km^2 and 9.09 km^2, respectively, indicating a concentration of development within thermally intensified zones. Water bodies exhibit a moderate negative correlation with LST (r = -0.53), as indicated in the regression equation y = -0.2831x + 1.8245 and an R^2 of 0.2817. Although the overall area of water bodies is relatively limited, their spatial distribution tends to coincide with lower-temperature zones, reflecting their role in thermal regulation through evaporative cooling. Open land also shows a negative correlation with LST (r = -0.48), as indicated by the regression model y = -1.3064x + 8.9601, with an R^2 of 0.2296. The reduction of open land in higher-temperature zones may indicate ongoing land conversion to built-up areas, contributing to the overall increase in surface temperatures. In summary, the regression patterns observed in 2013 strongly suggest that the expansion of built-up land principally drives the rise in LST, while vegetated and water-covered areas contribute to thermal mitigation (Table 11 & Fig. 14).

Table 11. Correlation of Land Cover to Land Surface Temperature (LST) in 2013

	TAHUN 2013				
	LST (°C)	Water Bodies	Built-up Land	Bare Land	Vegetation
		KM²			
1	<25 °C	0.74	0.52	2.88	11.44
2	25,1-28°C	2.37	2.89	11.44	49.56
3	28,1-30°C	1.10	2.24	6.91	19.82
4	30,1-32°C	0.32	10.61	3.81	11.19
5	>32 °C	0.35	9.09	0.16	2.95
	correlation (r)	**-0.53**	**0.88**	**-0.48**	**-0.48**

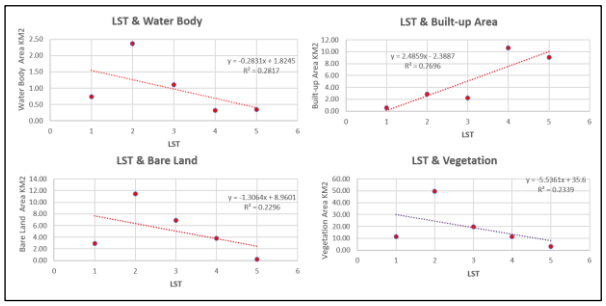

Fig 14. Graph of the Influence of Land Cover on Land Surface Temperature (LST) 2013

Based on the analysis of the relationship between land cover types and Land Surface Temperature (LST) in 2023, variations in surface temperature were found to be significantly associated with the dominant land cover categories. Vegetation dominated the lower temperature ranges of <25 °C and 25.1–28 °C, with respective areas of 25.66 km^2 and 39.38 km^2. As temperatures increased, vegetation cover decreased sharply, with only 1.79 km^2 recorded in the range of> 32 °C. A robust negative correlation was observed between vegetation and LST (r = -0.80), as indicated by the regression equation y = -8.5536x + 45.006, with R^2 = 0.6388. This suggests a strong tendency for surface temperatures to decrease as vegetation cover increases, reinforcing vegetation's role in providing shade, enhancing evapotranspiration, and mitigating urban heat through thermal buffering. In contrast, built-up land

exhibited the opposite trend. The highest area was recorded in the 28.1–30 °C category (16.18 km^2), with a considerable extent in the >32 °C category (9.86 km^2). The moderate positive Correlation (r = 0.44) is reflected in the regression equation y = 1.5204x + 3.1362. However, the relatively low R^2 value of 0.194 suggests that additional factors,s such as surface materials, building morphology, and microclimate characteristics,s may also influence surface temperatures in urbanized zones.

Bare land was mainly concentrated within the moderate temperature classes (25.1–30 °C), with the highest extent of 4.08 km^2 at 25.1–28 °C. A strong negative correlation (r = -0.76) with LST is represented by the regression model y = -0.954x + 5.0654, with R^2 = 0.5831, indicating that a reduction in bare land, likely due to land conversion, is associated with increased surface temperatures. Meanwhile, water bodies, though covering relatively small areas, were mainly found in the lower to moderate temperature categories (<28 °C), peaking at 1.90 km^2 in the 25.1–28 °C range. A mild negative correlation (r = -0.62) with LST is observed in the regression equation y = -0.2866x + 1.6898, yielding an R^2 of 0.3808, which highlights the contribution of water bodies in stabilizing surface temperatures through their natural cooling effects (Table 12 and Fig. 15).

Table 12. Correlation of Land Cover to Land Surface Temperature (LST) in 2023

		TAHUN 2023			
	LST (⁰C)	Water Bodies	Built-up Land	Bare Land	Vegetation
		KM²			
1	<25 °C	0.70	2.35	2.84	25.66
2	25,1-28°C	1.90	4.95	4.08	39.38
3	28,1-30°C	1.19	16.18	3.89	28.31
4	30,1-32°C	0.30	5.15	0.19	1.58
5	>32 °C	0.06	9.86	0.02	1.79
	correlation (r)	-0.62	0.44	-0.76	-0.80

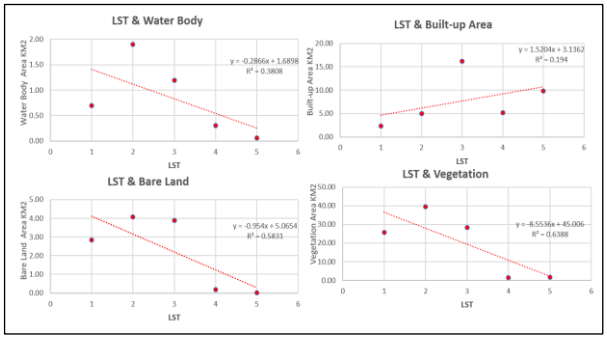

Fig 15. Graph of the Influence of Land Cover on Land Surface Temperature (LST) 2023

Land cover changes from 2003 to 2023 significantly influenced surface temperature dynamics. Vegetation consistently played a cooling role, with areas of dense vegetation tending to have lower surface temperatures. Conversely, the decline in vegetation over time, which aligns with rising temperatures, indicates that reduced vegetation directly contributes to higher surface temperatures. Built-up areas exhibited an inverse relationship: greater urban development intensity was associated with higher temperatures, particularly during the early analysis period. However, in recent years, the impact of built-up land on temperature has weakened, suggesting the possibility of other environmental interventions. Bare land and water bodies also contributed to temperature regulation, though their effects varied over time. These findings confirm that the conversion of vegetated land into built-up areas is a key factor in the rise of surface temperatures in Tanjungpinang City.

The findings of this study provide important insights for future research, spatial planning, and urban policy development in coastal cities such as Tanjungpinang. The consistent expansion of built-up land, accompanied by a marked decline in vegetation cover, demonstrates that urban growth has occurred with limited consideration of thermal and ecological balance. This pattern highlights the need for land-use planning strategies that explicitly integrate thermal environmental indicators, such as Land Surface Temperature (LST), into zoning regulations and development control mechanisms. Incorporating LST as an ecological constraint can help planners identify priority areas for green space preservation and urban heat mitigation. At the district level, the contrasting land cover and LST characteristics indicate differentiated planning needs. Districts with intense urbanization, such as Tanjungpinang Barat and Tanjungpinang Timur, require immediate interventions through the expansion of urban green infrastructure, including urban parks, street trees, and green roofs, to reduce surface heat accumulation. In contrast, districts that still retain relatively extensive vegetation, such as Tanjungpinang Kota and parts of Bukit Bestari, should be prioritized as ecological buffer zones, where land conversion is carefully restricted to maintain thermal stability.

From a policy perspective, the strong negative Correlation between vegetation cover and LST confirms the effectiveness of green spaces as a climate adaptation measure. This evidence supports formulating policies that mandate minimum green space ratios in urban development projects and encourage nature-based solutions as part of climate-resilient urban planning. Furthermore, the spatially uneven distribution of heat highlights the importance of district-specific policies rather than uniform citywide regulations. For future research, the results suggest that integrating additional variables such as building density, surface material characteristics, and urban morphology would enhance understanding of urban thermal dynamics. Overall, this study demonstrates that land cover management plays a critical role in controlling surface temperatures, and its findings can provide a scientific basis for sustainable spatial planning and policy formulation to mitigate urban heat stress in rapidly developing coastal cities.

4. Conclusion

This study reveals that over the past two decades (2003–2023), significant changes in land cover have occurred in Tanjungpinang City. Built-up land expanded by 27.15 km^2, indicating rapid urban development, while vegetation cover declined by 14.02 km^2, reflecting a consistent reduction in green space. Bare land initially increased by 1.45 km^2 during the first decade but then sharply declined, resulting in a net decrease of 12.74 km^2. Water bodies also decreased slightly by 0.39 km^2, suggesting environmental pressure on aquatic ecosystems. These land cover changes directly impacted land surface temperature (LST). The very high-temperature category (>32°C) grew from 0.82 km^2 to 6.46 km^2, while the very low-temperature category (<25°C) decreased by 10.89 km^2. This trend highlights a clear link between vegetation loss and temperature rise, as well as the role of urban expansion in increasing thermal intensity. Areas with low

temperatures were predominantly vegetated, while high-temperature zones were dominated by built-up land.

Regression analysis reinforces these findings. In 2023, vegetation exhibited a strong negative correlation with LST (r = -0.80), indicating that increased vegetation cover effectively reduces surface temperature through processes such as evapotranspiration and solar radiation absorption. Built-up areas showed a positive correlation with LST (r = 0.44), although weaker compared to previous years, suggesting that urban surfaces continue to contribute to heat buildup. Bare land and water bodies also showed negative correlations with LST, but their influence appeared to vary over time and across spatial distributions. Overall, the findings confirm that the conversion of vegetated areas into built-up land is the primary driver of surface temperature increases in Tanjungpinang City.

Suggestions for future research include conducting direct measurements of surface temperature in the field to improve the accuracy of satellite-based LST interpretation. These field observations can serve as essential comparison data to enhance the accuracy of the analysis and deepen the understanding of temperature changes. Additionally, it is recommended to include more variables in the statistical analysis to make the research results more comprehensive and in-depth.

Acknowledgements

The Author would like to express sincere gratitude to all parties who have provided support throughout the research on the Influence of Land Cover Change on the Spatial Distribution of Land Surface Temperature in Tanjungpinang City. The Author also extends heartfelt thanks to fellow researchers from the University of Maritime Raja Ali Haji (UMRAH) for their valuable contributions and collaboration during the study. References.

References

Adeyeri, O. E., Zhou, W., Ndehedehe, C. E., & Wang, X. (2024). Global vegetation, moisture, thermal, and climate interactions intensify compound extreme events. Science of the Total Environment, 912(December 2023), 169261. https://doi.org/10.1016/j.scitotenv.2023.169261

Ahmad, M. N., Shao, Z., & Javed, A. (2023). Modelling land use/land cover (LULC) change dynamics, prospects, and their environmental impacts based on geospatial data models and remote sensing data. Environmental Science and Pollution Research, 30(12), 32985–33001. https://doi.org/10.1007/s11356-022-24442-2

Alexander, C. (2020). Normalised difference spectral indices and urban land cover as indicators of land surface temperature (LST). International Journal of Applied Earth Observation and Geoinformation, 86(November 2019), 102013. https://doi.org/10.1016/j.jag.2019.102013

Alfiansyah, M., Nuarsa, I. W., & Brasika, I. B. M. (2023). Perbandingan Beberapa Metode Klasifikasi Menggunakan Citra Landsat dan Sentinel Untuk Pemetaan Sebaran Mangrove Di Kawasan Ekowisata Mangrove PIK Jakarta Utara. Journal of Marine and Aquatic Sciences, 9(1), 82. https://doi.org/10.24843/jmas.2023.v09.i01.p09

Alisjahbana, A. S., & Murniningtyas, E. (2018). TUJUAN PEMBANGUNAN BERKELANJUTAN DI INDONESIA: KONSEP, TARGET DAN STRATEGI IMPLEMENTASI. In Unpad Press.

Ally, H., Wahyuningtyas, J., & Rahmadana, M. I. (2024). Analisis Spatio temporal Pengaruh Aktivitas industri terhadap fenomena UHI dan LST di Kota Jakarta Timur. ENVIRO: Journal of Tropical Environmental Research, 26(1), 26. https://doi.org/10.20961/enviro.v26i1.93086

Anasiru, R. H. (2016). Spatial Analysis in the Classification of Critical Land in The Sub-Basin of Langge Gorontalo. Jurnal Informatika Pertanian, 25(2), 261–272. https://repository.its.ac.id/72342/1/3612100033-undergraduate-theses-.pdf

Bogaert, J., Vranken, I., & Andre, M. (2014). Biocultural Landscapes. Biocultural Landscapes. https://doi.org/10.1007/978-94-017-8941-7

BPS Tanjungpinang. (2023). Kota Tanjungpinang Dalam Angka 2024. In Badan Pusat Statistik. BPS Kota Tanjungpinang/BPS-Statistics Tanjungpinang Municipality. https://web-api.bps.go.id/download.php?f=NtyzP9ku/rnPo4EW/d50/XJ1bndockFFWlRBQ1hxQTFnSk8xcjBoT0FMMVRUS09NdHBXaFMrVG5OeUQ0a2xucnRvT0pXUlprOWQ5U3J5eE00cGtGZ3UwOS9nTXBlTGFXSVg0a3M2emZIQmU4QmkwdkVYSE5BZGQ3WjFwVmdqN3lJWkZiUTFwT2NOanJSRldOZXhzVG9GODI0WXo3Q3o3bl

Chatterjee, U., & Majumdar, S. (2022). Impact of land use change and rapid urbanization on urban heat island in Kolkata city: A remote sensing based perspective. Journal of Urban Management, 11(1), 59–71. https://doi.org/10.1016/j.jum.2021.09.002

Cheval, S., Amihăesei, V. A., Chitu, Z., Dumitrescu, A., Falcescu, V., Irașoc, A., Micu, D. M., Mihulet, E., Ontel, I., Paraschiv, M. G., & Tudose, N. C. (2024). A systematic review of urban heat island and heat waves research (1991–2022). Climate Risk Management, 44(March). https://doi.org/10.1016/j.crm.2024.100603

Eboy, O. V., & Kemarau, R. A. (2023). Analysis of Extreme Heat Land Surface Temperature at a Tropical City (1988-2022): A Study on the Variability of Hot Spot during El Niño Southern Oscillation (ENSO). Science and Technology Indonesia, 8(3), 388–396. https://doi.org/10.26554/sti.2023.8.3.388-396

Egorov, A. V., Hansen, M. C., Roy, D. P., Kommareddy, A., & Potapov, P. V. (2015). Image interpretation-guided supervised classification using nested segmentation. Remote Sensing of Environment, 165, 135–147. https://doi.org/10.1016/j.rse.2015.04.022

Farnaz, Nuthammachot, N., & Ali, M. Z. (2025). Comparative study of multiple algorithms classification for land use and land cover change detection and its impact on local climate of Mardan District, Pakistan. Environmental Challenges, 18(December 2024), 101069. https://doi.org/10.1016/j.envc.2024.101069

Fathoni, M. A. (2025). Spatiotemporal analysis of land surface temperature and land cover change: Assessing the impact of urbanization and vegetation dynamics. Spatial Review for Sustainable Development, 2(1), 21–37. https://journal-iasssf.com/index.php/SRSD/article/view/1752

Gomaa, M. M., Nabil, J., Berkouk, D., & Ragab, A. (2025). A Comparative Study of Vegetation Strategies for Outdoor Thermal Comfort in High- and Low-Density Urban Areas. Urban Science, 9(10), 1–30.

https://doi.org/10.3390/urbansci9100416
Guha, S., & Govil, H. (2020). Land surface temperature and normalized difference vegetation index relationship: a seasonal study on a tropical city. SN Applied Sciences, 2(10), 1–14. https://doi.org/10.1007/s42452-020-03458-8
Handayani, M. N., Sasmito, B., & Putra, A. (2017). ANALISIS HUBUNGAN ANTARA PERUBAHAN SUHU DENGAN INDEKS KAWASAN TERBANGUN MENGGUNAKAN CITRA LANDSAT (STUDI KASUS : KOTA SURAKARTA). Jurnal Geodesi Undip, 6(4), 517–525. https://doi.org/https://doi.org/10.14710/jgundip.2017.18145
Hermosilla, T., Wulder, M. A., White, J. C., & Coops, N. C. (2022). Land cover classification in an era of big and open data: Optimizing localized implementation and training data selection to improve mapping outcomes. Remote Sensing of Environment, 268, 112780. https://doi.org/10.1016/j.rse.2021.112780
Irawandani, T. D., Dipareza, A., & Hermana, J. (2018). The effect of land cover change on surface temperature based on satellite imagery in 30 cities in Indonesia. EnvironmentAsia, 11(1), 100–111. https://doi.org/10.14456/ea.2018.8
Jannah, G. S., & Bioresita, F. (2023). Pemantauan Land Surface Temperature (LST) dan Kaitannya dengan Tutupan Lahan (Studi Kasus: Kota Surabaya Tahun 2014-2022). Jurnal Teknik ITS, 12(2). https://doi.org/10.12962/j23373539.v12i2.122579
Kafy, A. Al, Dey, N. N., Al Rakib, A., Rahaman, Z. A., Nasher, N. M. R., & Bhatt, A. (2021). Modeling the relationship between land use/land cover and land surface temperature in Dhaka, Bangladesh using CA-ANN algorithm. Environmental Challenges, 4(June), 100190. https://doi.org/10.1016/j.envc.2021.100190
Kalamkar, S., & Geetha Mary, A. (2023). Multimodal image fusion: A systematic review. Decision Analytics Journal, 9(August), 100327. https://doi.org/10.1016/j.dajour.2023.100327
Kausarian, H., Septio, G., Sumantyo, J. T. S., Tutuko, P., Suryadi, A., & Mairizki, F. (2023). Landslide Vulnerability Identification Based on the Geological Condition, GIS Calculation, and Field Validation in the Tropical Area. Evergreen, 10(4), 2423–2438. https://doi.org/10.5109/7161458
Kurniantoro, R., Sasmito, B., & Hadi, F. (2023). Analisis Pengaruh Perubahan Kawasan Terbangun Menggunakan Algoritma Endisi Terhadap Suhu Permukaan Tanah. Jurnal Geodesi Undip, 12.
Livada, Č., Glavaš, H., Baumgartner, A., & Jukić, D. (2023). The Dangers of Analyzing Thermographic Radiometric Data as Images. Journal of Imaging, 9(7). https://doi.org/10.3390/jimaging9070143
Lu, D., Mausel, P., Batistella, M., & Moran, E. (2003). Comparison of land-cover classification methods in the Brazilian Amazon basin. Photogrammetric Engineering and Remote Sensing, 70(6), 723–731. https://doi.org/10.14358/PERS.70.6.723
Mohamed, A., Lorestani, N., & Shabani, F. (2025). Impact of urbanization on land surface temperature: A global perspective. Current Research in Environmental Sustainability, 10(October), 100315. https://doi.org/10.1016/j.crsust.2025.100315
Moraes, D., Campagnolo, M. L., & Caetano, M. (2024). Training data in satellite image classification for land cover mapping: a review. European Journal of Remote Sensing, 57(1). https://doi.org/10.1080/22797254.2024.2341414
Noviani, R., Saputra, A. E., Wijayanti, P., & Koesoma, S. (2024). Analysis of Land Use Land Cover and Land Surface Temperature in Karst Area: A Case Study Wonogiri Regency. Indonesian Journal of Applied Physics, 14(1), 89. https://doi.org/10.13057/ijap.v14i1.79048
Nurwanda, A., & Honjo, T. (2020). The prediction of city expansion and land surface temperature in Bogor City, Indonesia. Sustainable Cities and Society, 52, 101772. https://doi.org/https://doi.org/10.1016/j.scs.2019.101772
Ouria, M., Almeida, A., Yaghoubi Kondelaji, S., Moura, P., & de Almeida, A. T. (2025). Sustainable urban mitigation strategies regarding heat-related mortalities and thermal discomfort: an overview and comparative analysis. In Theoretical and Applied Climatology (Vol. 156, Issue 6). https://doi.org/10.1007/s00704-025-05477-0
Rangel-Peraza, J. G., Sanhouse-García, A. J., Flores-González, L. M., Monjardín-Armenta, S. A., Mora-Félix, Z. D., Rentería-Guevara, S. A., & Bustos-Terrones, Y. A. (2024). Effect of land-use and land-cover changes on land-surface warming in an intensive agricultural region. Journal of Environmental Management, 371, 123249. https://doi.org/https://doi.org/10.1016/j.jenvman.2024.123249
Rosandi, V. B., Pravitasari, A. E., & Rachendra, A. S. (2024). The Dynamics of Land Cover Change and Level of Sustainability Development in Depok City. Jurnal Pengembangan Kota, 12(1), 35–49. https://doi.org/10.14710/jpk.12.1.35-49
Saputri, D. R., Afriadi, A., Hilmi, N., Chidmahdjati, A. B., & Apriyenson, H. (2025). Identifikasi Perkembangan Lahan Terbangun di Kota Tanjung Pinang Tahun 2004-2024. Jural Riset Rumpun Ilmu Teknik, 4(2), 481–490. https://doi.org/10.55606/jurritek.v4i2.6136
Seyam, M. M. H., Haque, M. R., & Rahman, M. M. (2023). Identifying the land use land cover (LULC) changes using remote sensing and GIS approach: A case study at Bhaluka in Mymensingh, Bangladesh. Case Studies in Chemical and Environmental Engineering, 7(November 2022), 100293. https://doi.org/10.1016/j.cscee.2022.100293
Siregar, D. C., Ardah, V. P., & Ninggar, R. D. (2019). Identifikasi Kenyamanan Kota Tanjungpinang Berdasarkan Indeks Panas Humidex. Jurnal Ilmu Lingkungan, 17(2), 316. https://doi.org/10.14710/jil.17.2.316-322
Stamou, A., Dosiou, A., Bakousi, A., Karachaliou, E., Tavantzis, I., & Stylianidis, E. (2025). Assessing Spatial Correlations Between Land Cover Types and Land Surface Temperature Trends Using Vegetation Index Techniques in Google Earth Engine: A Case Study of Thessaloniki, Greece. Remote Sensing, 17(3). https://doi.org/10.3390/rs17030403
Sudjana, L., Sodikin, & Astarika, R. (2024). Spatial analysis of mangrove cover change and land suitability for its rehabilitation in Tanjungpinang City, Riau Islands Province, Indonesia. AACL Bioflux, 17(6), 2905–2921.
Voogt, J. A., & Oke, T. R. (2003). Thermal remote sensing of urban climates. Remote Sensing of Environment,

86(3), 370–384. https://doi.org/https://doi.org/10.1016/S0034-4257(03)00079-8

Vujovic, S., Haddad, B., Karaky, H., Sebaibi, N., & Boutouil, M. (2021). Urban Heat Island: Causes, Consequences, and Mitigation Measures with Emphasis on Reflective and Permeable Pavements. CivilEng, 2(2), 459–484. https://doi.org/10.3390/civileng2020026

Wahyudi, A. J., Afdal, Prayudha, B., Dharmawan, I. W. E., Irawan, A., Abimanyu, H., Meirinawati, H., Surinati, D., Syukri, A. F., Yuliana, C. I., & Yuniati, P. I. (2018). Carbon sequestration index as a determinant for climate change mitigation: Case study of Bintan Island. IOP Conference Series: Earth and Environmental Science, 118(1). https://doi.org/10.1088/1755-1315/118/1/012050

Wang, J., Jiang, C., Yang, G., Bai, G., & Yu, S. (2023). Study on thermal health and its safety management mode for the working environment. Frontiers in Public Health, 11(August), 1–11. https://doi.org/10.3389/fpubh.2023.1227630

Wang, S. W., Munkhnasan, L., & Lee, W. K. (2021). Land-use and land-cover change detection and prediction in Bhutan's high-altitude city of Thimphu using cellular automata and Markov chains. Environmental Challenges, 2(November 2020). https://doi.org/10.1016/j.envc.2020.100017

Wulder, M. A., Roy, D. P., Radeloff, V. C., Loveland, T. R., Anderson, M. C., Johnson, D. M., Healey, S., Zhu, Z., Scambos, T. A., Pahlevan, N., Hansen, M., Gorelick, N., Crawford, C. J., Masek, J. G., Hermosilla, T., White, J. C., Belward, A. S., Schaaf, C., Woodcock, C. E., … Cook, B. D. (2022). Fifty years of Landsat science and impacts. Remote Sensing of Environment, 280(April), 113195. https://doi.org/10.1016/j.rse.2022.113195

Yoo, C., Im, J., Cho, D., Yokoya, N., Xia, J., & Bechtel, B. (2020). Estimation of all-weather 1 km MODIS land surface temperature for humid summer days. Remote Sensing, 12(9), 1–23. https://doi.org/10.3390/RS12091398

Zhang, F., Zhang, X., Chen, W., Yang, B., Chen, Z., Tang, H., Wang, Z., Bi, P., Yang, L., Li, G., & Jia, Z. (2022). Cloud-Free Land Surface Temperature Reconstructions Based on MODIS Measurements and Numerical Simulations for Characterizing Surface Urban Heat Islands. IEEE Journal of Selected Topics in Applied Earth Observations and Remote Sensing, 15, 6882–6898. https://doi.org/10.1109/JSTARS.2022.3199248

Zhao, K., Jin, B., Fan, H., Song, W., Zhou, S., & Jiang, Y. (2019). High-performance overlay analysis of massive geographic polygons that considers shape complexity in a cloud environment. ISPRS International Journal of Geo-Information, 8(7). https://doi.org/10.3390/ijgi8070290

Zhu, K., Cheng, Y., Zhou, Q., Kápolnai, Z., & Dávid, L. D. (2023). The contributions of climate and land-use/land-cover changes to water yield services across geographic scales. Heliyon, 9(10). https://doi.org/10.1016/j.heliyon.2023.e20115